PCCP

Accepted Manuscript

ROYAL SOCIETY OF CHEMISTRY

www.rsc.org/pccp

Journal Name

ARTICLE

Thermal stability and hcp-fcc allotropic transformation in supported Co metal catalysts probed near operando by ferromagnetic NMR

Received 00th January 20xx,
Accepted 00th January 20xx

DOI: 10.1039/x0xx00000x

www.rsc.org/

Andrey S. Andreev[a,b,c], Jean-Baptiste d'Espinose de Lacaillerie†,[c], Olga B. Lapina[a,b], Alexander Gerashenko[d]

Despite the fact that cobalt based catalysts are used at the industrial scale for Fischer-Tropsch synthesis, it is not yet clear which cobalt metallic phase is actually at work under operando conditions and what is its state of dispersion. As it turns out, the different phases of metallic cobalt, fcc and hcp, give rise to distinct ferromagnetic nuclear magnetic resonance. Furthermore, within one Co metal particle, the occurrence of several ferromagnetic domains of limited sizes can be evidenced by the specific resonance of Co in multi-domain particles. Consequently, by ferromagnetic NMR, one can follow quantitatively the sintering and phase transitions of dispersed Co metal particles in supported catalysts near operando conditions. The minimal size probed by ferromagnetic Co NMR is not precisely known but is considered to be in the order of 10 nm for supported Co particles at room temperature and increases to about 35 nm at 850K. Here, in Co metal Fischer-Tropsch Synthesis catalysts supported on β-SiC, the resonances of the fcc multi-domain, fcc single-domain and hcp Co were clearly distinguished. A careful rationalization of their frequency and width dependence on temperature allowed a quantitative analysis of the spectra in the temperature range of interest, thus reflecting the state of the catalysts in near operando conditions that is without the uncertainty associated with prior quenching. The allotropic transition temperature was found to start at 600-650K, which is about 50K below the bulk transition temperature. The phase transition was fully reversible and a significant part of the hcp phase was found to be stable up to 850K. This anomalous behavior that was observed without quenching might prove to be crucial to understand and model active species not only in catalysts but also in battery materials.

[a] *Pirogova str. 2, Novosibirsk State University (NSU), Novosibirsk, 630090, Russia*
[b] *Pr. Lavrentieva 5, Solid-State NMR group, Boreskov Institute of Catalysis SB RAS (BIC SB RAS), Novosibirsk, 630090, Russia*
[c] *10 Rue Vauquelin, Soft Matter Sciences and Engineering (SIMM), UMR CNRS 7615, PSL Research University, ESPCI ParisTech, Paris, 75005, France*
[d] *S. Kovalevskoy str. 18, Kinetic Phenomena laboratory, Institute of Metals Physics UB RAS, Ekaterinburg, 620041, Russia*

† * jean-baptiste.despinose@espci.fr
Electronic Supplementary Information (ESI) available: [details of any supplementary information available should be included here]. See DOI: 10.1039/x0xx00000x

Journal Name

ARTICLE

Introduction

Today, Fischer-Tropsch Synthesis (FTS) on cobalt is used in many countries as a key process for gas-to-liquids (GTL) technology.[1–3] The most recent developments focus on biomass conversion to produce lower olefins (C_2-C_6).[4–6] The current state of knowledge has been reviewed[7,8] and it is still not totally clear what Co phases are at play in the catalyst. The metallic phase is usually supported on oxides but composites and SiC are promising alternatives due to their higher thermal conductivity.[9–12] Unfortunately, the structural characterization of the Co FTS catalysts are performed at ambient or low temperature, mostly by XRD and TEM, and it is not certain that they accurately describe the state of the catalyst under actual reaction temperature conditions. Recently, Co FTS catalysts have been characterized by ^{59}Co nuclear magnetic resonance (NMR)[13–15] but this technique was performed at temperatures differing from the operating ones.

In a broader context than catalysis, the phase diagram of bulk Co metal is well known. In particular, the transition from hcp to fcc stacking has been studied in detail through various techniques[16–19] including ^{59}Co NMR in the absence of an applied external magnetic field.[20,21] This method takes advantage of the fact that Co metal is ferromagnetic in a wide range of temperatures and particle sizes thus allowing the recording of the NMR signal of the sample in its internal field.[22] The magnetic behaviour related to the hcp to fcc phase transition has been investigated by NMR in the bulk,[20] as well as in micron size powders after heating and quenching.[21] However, nanosize Co metal particles have never been studied above room temperature by NMR. At first sight, this might be surprising since in principle NMR is much more efficient for phase determination than XRD for small crystal sizes, but actually the complex temperature dependence of the ferromagnetic NMR signal renders quantitative phase analysis intricate. In the bulk, below ~ 693K, the stable phase for Co metal is hcp but for nanosize Co metal particles both fcc and hcp Co metal stackings are observed even at ambient and low temperatures.[23–27] Kitakami et al.[28] have considered this anomaly by studying various Co polyhedra synthesized by sputtering and comparing the results to free energy minimization predictions. They observed a close relationship between the particle size and the crystal phase at room temperature. Pure fcc is found to be the dominant phase for particles of less than 20 nm in diameter, for ~ 30 nm particles a mixture of both hcp and fcc phases are present, while particles over 40 nm crystallize as hcp with inclusion of a very small amount of fcc. The *in situ* phase identification of dispersed nanosize Co systems has some importance as the crystal phase of the particles is expected to affect important properties such as catalytic activity[2,4] or battery charge cycles.[29,30] Concerning supported catalysts, only several early attempts have been made by ^{59}Co NMR in such catalysts,[13–15] although a renewed interest has occurred recently.[9,11,31,32] In fact, the majority of the ^{59}Co NMR studies to date have been performed at low temperatures (4.2K), and only few results are reported at room temperatures. The choice of operating at a low temperature is logical as it gives a high enhancement of the NMR signal and opens in particular the possibility to studying superparamagnetic cobalt particles[33] when applying a weak external magnetic field. Nevertheless, cobalt nanoparticles are used most of the time at, or well above, room temperature (for example, the Fischer-Tropsch synthesis takes place at 473-513K for the so-called low temperature processes and 573-623K for the high temperature ones,[1] and there is a need to bridge the experimental gap between measurements performed at high, ambient and low temperatures. Consequently, the present study is an *in situ* examination by ferromagnetic ^{59}Co NMR of the temperature stability and the hcp-fcc allotropic transition in supported Co metal nanoparticles.

Experimental

A sample of Co metal supported on β-SiC (15 wt.% of Co) was prepared by conventional Co nitrate impregnation technique followed by calcination under air at 623K for 4 hours. Subsequently, the sample was reduced under an H_2 flow in a U-shape glass reactor. 0.5 g of the sample was sealed on-line to prevent Co metal oxidation in 5-mm outer diameter tubes. A residual Ar pressure of 70 Torr was kept in the ampoule to maintain heat conductance. The sealed tube was then cooled down and transferred into the solenoid of a commercial special design Bruker broadband static high-temperature 5-mm probe. The temperature was raised “in situ” to the one of interest for the NMR measurement by means of a heater, which surrounded the acquisition coil. A ceramic protection covered the heating part and the coil. The term “in situ” indicated that the heating was performed inside the NMR probe and that all spectra were acquired at high temperature, and at room temperature after by quenching in liquid nitrogen as was previously done by Speight et al.[21] In that sense, the NMR signal was acquired in situ with respect to the hcp-fcc phase transition and near operando with respect to the

catalyst activation procedure. All ferromagnetic NMR experiments were carried out using a Bruker Avance III 500 MHz console but the experiments were performed outside of the magnet, thus without application of any external magnetic field. Note that all measurements took place on a single sample and using the same detection coil at a fixed amplifier output power, thus insuring that the intensity of the radiofrequency (rf) field was constant. In this manner, the intensities of all the spectra could be compared meaningfully. The spectra were obtained by summing Fourier transformed spin echoes acquired with 500 kHz carrier frequency steps as described elsewhere.[34] Such large steps can be used because the quality factor of the rf circuit is considerably degraded by the presence of the magnetic sample thus making the circuit less frequency selective and providing a bandwidth of ~ 2 MHz. Two equal RF pulses (~ 40 W at the output of the amplifier) of 0.3 µs duration with an interpulse delay of 7 µs were implemented to generate each spin-echo. The sequence repetition rate was 300 Hz, and the number of transients was varied from 1000 to 30000 depending on the signal intensity. Frequency tuning was insured by means of a home-made auto-tune device developed by one of us in Ekaterinburg. It is based on two step motors and a controller using the wobble curve exported from the Bruker Topspin software as an input. The peak positions, intensities and width were obtained by decomposition into Gaussian lineshapes. No corrections for the enhancement factors were performed due to experimental limitations. Accurate measurements of correction factors require additional power variations (at least 5 values), thus increasing the total measurement time to about 60 hours in the present case. Unfortunately the probe could not sustain such a long continuous high temperature heating without damage. Not using correction factors was not a limitation though as only relative variations from one temperature to the next was considered in the present study. Nevertheless, the enhancement factor was measured at room-temperature. Accordingly, it was estimated that the intensities reported here without corrections overestimated the fcc multi-domain resonances by a factor of 2. The basics of ferromagnetic NMR theory are summarized in the Supplementary materials. Likewise, the supporting characterization of the sample by powder XRD and HRTEM can be found in the Supplementary materials.

It must be understood that since the experiments were carried out at high temperatures, not all Co metal particles were NMR visible. The blocking temperature of the ferromagnetic domains depends on the size of the particles and, below a critical size, at a given temperature, the particles are superparamagnetic and thus invisible by NMR. The actual value of the critical size is not fully known and depends on the particle shape. The critical size at room temperature for Co particles has been reported to be above 23 nm.[32] However, in a recent PhD thesis[35] it was shown experimentally that 10 nm size particles were visible by internal field ^{59}Co NMR at room temperature. Furthermore, using the calculations of Liu et al.,[32] a critical size of ~34 nm at 850K can be estimated. It can thus be concluded that in the temperature range of the present study, the critical size below which the particles become NMR invisible varies from about 10 to 35 nm going from room temperature to 850K. These values can be considered as conservative.

Results and discussion

Identification of the resonances of the hcp and fcc phases

The temperature study by ferromagnetic NMR of nanosize Co metal clusters supported on β-SiC is presented in Figure 1. First of all, as expected, the spectra shifted globally to lower frequency with the temperature increase due to the reduction of the electronic magnetization *M* (see discussion on the ferromagnetic signal and its temperature dependence in the Supplementary materials). Nevertheless, the spectra contained all the same features, namely three resonances attributed to fcc multi-domains particles, fcc single-domain particles and hcp Co in agreement with the literature data.[36–41] The lower frequency resonance is ascribed to the signal from fcc multi-domains (m. d.) and the middle one to fcc single-domain (s.d.) particles.

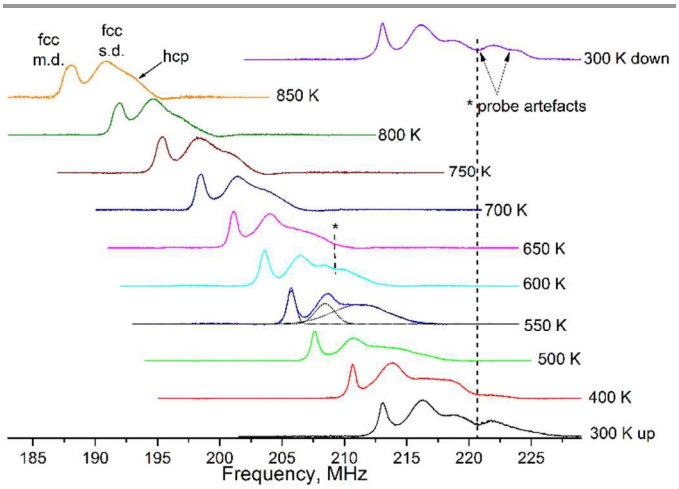

Fig. 1 Ferromagnetic ^{59}Co NMR spectra at variable temperatures in supported metal cobalt nanoparticles. Intensities are normalized to their maxima.

The frequency shift between the multi-domain and the single-domain fcc arises from the contribution of the demagnetization field to the local field in single-domain particles. As the depolarization tensor depends on the shape of the single-domain particles, which is distributed, the resonance of the single-domain particles is expected to be broader than the one from the multi-domains. This was indeed the case.

The large high frequency line at highest frequency was attributed to the hcp phase. In contrast to what was observed here, in large (~ 10 µm) hcp monocrystals the spectrum is dominated by two well-resolved resonance lines that correspond to nuclei at the edge (214 MHz) and at the center

of domain walls (221 MHz). Both types of environments correspond to a magnetic field perpendicular to the c crystallographic axis at room temperature and the corresponding nuclei exhibit a significant rf enhancement factor of the domain walls η_w.[20,42–46] As a result, the resonance of the hcp domains is not visible as it is dominated by the contributions from the domain walls. However here, where the crystals are of nanometer sizes, the reduction of the crystal sizes and magnetic domains resulted in a considerable reduction of the enhancement factor of the domain walls η_w as explained by Portis and Gossard in their seminal work on nuclear resonances in ferromagnetic cobalt.[36] Consequently, in the part of the spectra arising from the hcp nanocrystals, the values of η_w and η_d (enhancement factor of the domains) became comparable and the contribution to the signal from the magnetic domain E_T^d became significant compared to the one of the domain walls E_T^w(eq. 4S and 5S). This contribution from the hcp domains was very broad due to the well-known large local field anisotropy in hcp crystal equal to 7 kOe.[20] Another reason for the breadth of this line was that, as for the fcc single-domains, variations of particle shapes result in an additional distribution of resonance frequencies. This point was supported by the fact that T_2 was measured to be within the range 10-20 µs, values that could not account for a FWHM of more than 1 MHz. The broadening was thus inhomogeneous, that is resulting from the local field dispersion.

Temperature dependence of the spectral characteristics: frequency, intensity and width

The resonances of the fcc cobalt in multi-domains, of the fcc cobalt single-domains, and of the hcp cobalt being identified, it was possible to study their respective temperature dependence. Indeed, in order to analyse the phase transformation in a quantitative manner, it is first necessary to take into account the temperature dependence of ferromagnetic NMR experimental parameters such as the resonance frequency, the echo intensities and their widths. As discussed in the Supplementary materials, these experimental parameters depended on the nuclear equilibrium magnetization, on the hyperfine field (proportional to the equilibrium electronic magnetization), either directly or through the enhancement factors η_w and η_d, and on the relaxation rates. Figure 2 shows the temperature dependence of the resonance frequency of all species presented in the spectra of Figure 1.

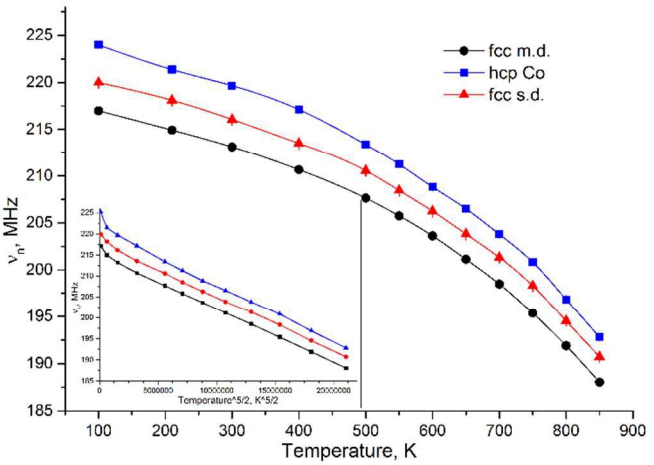

Fig. 2 Temperature dependence of the ferromagnetic NMR frequencies of the different Co species obtained by decomposition of Figure 1. Blue squares correspond to hcp Co, red triangles – to fcc single-domain (s. d.) Co, and black circles to fcc multi-domain (m.d.) Co.

In the expression of the ferromagnetic NMR frequency in equation (3S), the only term expected to depend on temperature is the equilibrium electronic magnetization *M*.

$$\Omega_n = 2\pi\nu_n(T) \propto M(T)$$

Since all measurements were performed well below the Curie temperature of cobalt (~ 1400K), the temperature evolution of this magnetization can be predicted safely by spin-waves theory. Keeping the first two terms of the expansion, one can write

$$\frac{\nu_n(0)-\nu_n(T)}{\nu_n(0)} = \frac{M(0)-M(T)}{M(0)} = \alpha T^{3/2} + \beta T^{5/2} \quad (1)$$

As seen from the insert in Figure 2, the deviation from the Bloch 3/2 law is small but led to measurable values of the *β* parameter that can be associated with the need for a more accurate energy expression in spin-waves theory or with spin waves interaction,[22] i.e. in our case the interparticles interaction. The values obtained for the fitting parameters *α* and *β* are reported in Table 1. The α and *β* parameters for the resonances from the fcc multi-domains and fcc single domains coincided within experimental errors. This was predictable as single and multi domain particles differ only by the dipolar demagnetization field.

Table 1. Parameter extracted from the fit of dependencies shown in Figure 2 for each observed line.

Parameter	fcc multi domain	fcc single domain	hcp
υ_0, MHz	217.2 (fixed)	220.0 ±0.3	223±0.3
α, $K^{-3/2}$	$(1.9\pm0.2)*10^{-6}$	$(1.8\pm0.2)*10^{-6}$	$(1.4\pm0.3)*10^{-6}$
β, $K^{-5/2}$	$(4.0\pm0.2)*10^{-9}$	$(4.1\pm0.2)*10^{-9}$	$(4.7\pm0.3)*10^{-9}$

The difference between the single domain and multi-domain resonances corresponds to the demagnetization field. Here, the 2.8 MHz for the fcc particles led to an estimate of 2.8 kOe. For a spherical particle, the dipolar field relates to the saturation magnetization M_s at 0K through

$$H_{di} = -4\pi/3 M_s$$

Leading to a saturation magnetization of 1.2 kG, a value very close to what is observed in bulk fcc Co.[47]

The frequency temperature dependence observed in the present work is compared with results of the literature in Figure 3 and Figure 4. From Figure 3, it can be seen that concerning fcc single domains, the present results differed significantly from the only previous report we could find which corresponded to an α value of $(4.87\pm0.2)*10^{-6}K^{-3/2}$ and an extrapolation to 0K at 222.2 MHz instead of 220MHz.[39] It is plausible though that the results obtained in the present study were of better quality due to experimental progress, the earlier work being performed with a continuous wave spectrometer. In such conditions, the broad line of fcc domain Co contains a mixture of absorption and dispersion signals preventing a precise determination of the line position.

On the other hand, the temperature evolution of the fcc multi-domain resonance was in agreement with all previously published studies[20,39,43] up to 400K (see Figure 4). It was noticeable though that the high-temperature part (up from 400K) of the temperature frequency dependence differed significantly from the ones previously observed on larger particles. At these temperatures, the evolution is dominated by the β parameter. It thus appeared that this parameter is more affected than α by the modification of the electronic structure due to particle size reduction. Finally, concerning the hcp resonance, the present work is to our knowledge the first one in nano-sized samples. Despite the fact that in bulk hcp Co several ferromagnetic NMR temperature studies were done,[20,43,44] in nanosize hcp Co the ferromagnetic NMR spectrum has been already reported several times[23,26,33,40] but never its temperature dependence which is crucial for catalytic studies.

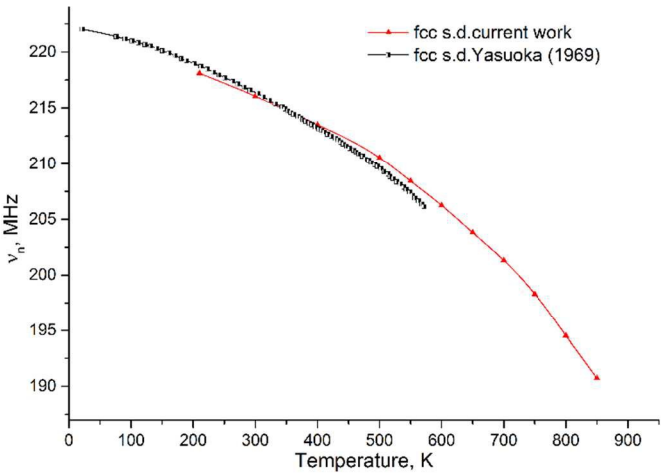

Fig. 3 Comparison with previous works on the magnetization temperature dependencies for fcc single domains (s.d.). Red triangles correspond to the fcc s.d. line of present work and semi-filled squares to data from Yasuoka et al.[39]

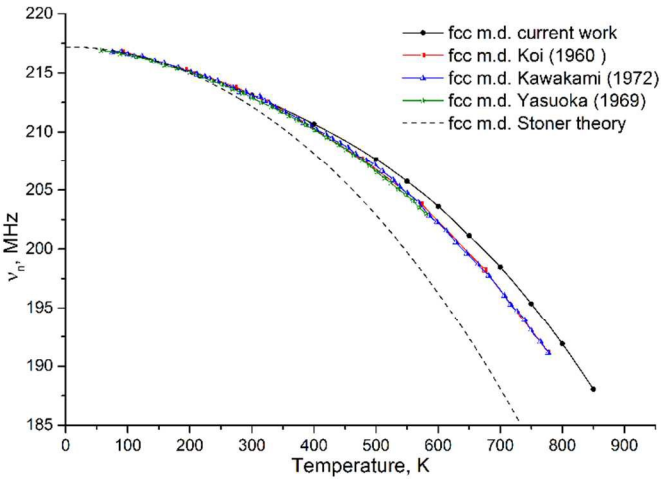

Fig. 4 Comparison with previous works on magnetization temperature dependencies for fcc multi-domain (d.w.) reported in different works. Black circles correspond to the fcc m.d. line in the current work, semi-filled red squares to the work of Koi et al.,[43] semi-filled blue triangles to Kawakami et al.,[20] semi-filled stars to Yasuoka et al.[39] and a dash line to Stoner's theory.[48]

The spectra of Figure 1 were represented with normalized intensities and thus the intensity drop with temperature was not pictured. The evolution of the absolute integrated intensities of each contribution to the spectra is plotted with respect to temperature in Figure 5. A drop of the overall intensity with temperature was observed.

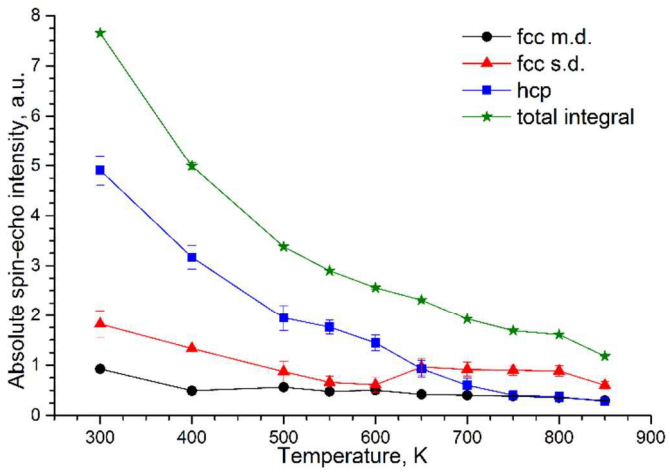

Fig. 5 Absolute integrated intensities temperature dependence. The blue squares correspond to hcp Co stacking, the red triangles to fcc single domain species, the black circles to fcc multi-domain (m.d.) resonance and the green stars to the sum of individual intensities.

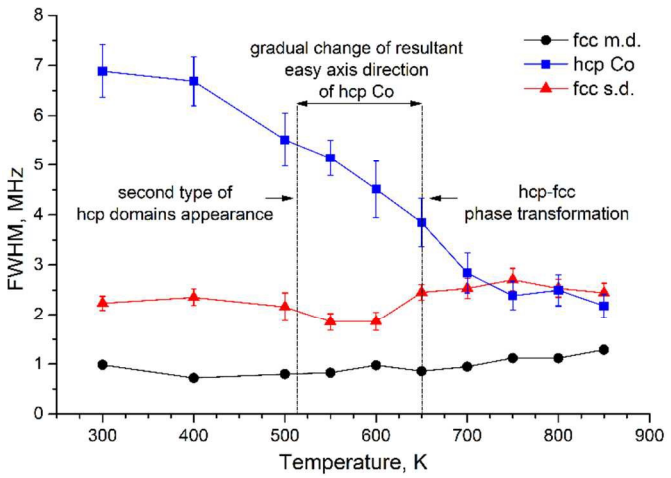

Figure 6. FWHM dependence on temperature. Blue squares correspond to hcp Co stacking, red triangles to fcc single domain species and black circles to fcc m.d. resonance.

The intensities of the Co resonances expressed in equation (4S) and (5S) are impacted in different ways by the temperature: transverse relaxation (T_2*), nuclear equilibrium magnetization (m) and enhancement factor (η_d), all vary with temperature in different ways but all such as to contribute to the decrease of the signal. The rate of relaxation can show complex variations with temperature reflecting the dependency of the various relaxation paths involved in the strongly coupled spin systems present in magnetically ordered materials,[49] but, in any case, the rate of relaxation is expected to increase with temperatures and as a consequence, at fixed echo time Δ, this contributed to the decrease of the echo intensity. Also, at high temperature, namely above 600K, the echo intensity can be further reduced by superparamagnetic relaxation due to increased reorientation of the magnetization.[24] As far as the nuclear equilibrium magnetization m is concerned, it is expected to decrease as 1/T. Finally, since the enhancement factors of both the domain and the domain wall scaled with the hyperfine field, itself approximated by $B_{hf} = \lambda_m m$ (where λ_m is the molecular field approximation parameter) a further intensity decrease according was expected for all lines (see Supplementary Materials).

Not only the resonance frequencies and echo intensities evolved with temperature but also their width, expressed as their full width at half maximum (FWHM) as shown in Figure 6. The most drastic changes occurred for the hcp Co resonance. Within a temperature region of 400-750K the FWHM was progressively cut in half. Therefore, this meant that the distribution of magnetic fields mainly responsible for FWHM in hcp Co (as discussed above) decreased drastically within this temperature range. Remarkably, hcp Co in known to have a magnetic transformation starting from ~ 513K, at which another type of hcp domains appears, and a gradual change of the easy axis direction of hcp Co occurs.[50] A further decrease could be attributed to the start of hcp-fcc Co metal allotropic phase transition as will be discussed below.

Allotropic hcp to fcc phase transformation in nanoparticles

The ultimate goal of this study was to evaluate the potential of ferromagnetic ^{59}Co NMR to study the hcp/fcc transformation in nanoparticles. If the nuclear (m) and electronic (M) equilibrium magnetization variations with temperature are expected to affect similarly the spin echo intensities of different phases, domains and walls, the same cannot be said a priori concerning the enhancement factors (η) and the transverse decay rates (T_2*). Consequently, a quantitative analysis of the phase evolution with temperature cannot be performed directly without precaution from the relative line intensities represented in Figure 5. In particular, it must be understood that the contribution of the smallest particles disappear progressively from the signal as they become superparamagnetic when the temperature rises. However, the relative contributions of all resonances varied little up to about 600K (Figure 7). This was a strong indication that no structural changes occurred below 600K. Going back to Figure 5, the temperature evolution of the intensity of the fcc s.d. resonance changed between 600 and 650K: the smooth decrease was interrupted, and a small increase could be observed. As explained above, for a given amount of spins in

particles of constant sizes, the echo intensity can only decrease with temperature. An increase can thus in all confidence only be attributed to a phase transition. Since the temperature changes in the spectra were fully reversible (Figure 7) and since no sintering was observed by high resolution TEM (not shown), it was thus concluded that the amount of nuclei in fcc s.d. increased, that is that a phase transition from hcp to fcc started to occur at this temperature. This is further illustrated in Figure 7 where the fcc to hcp ratio of the corresponding ferromagnetic ^{59}Co NMR resonances is plotted. Again, as no corrections for relaxation and enhancement factors were performed, this ratio is not quantitative. However, the occurrence of the gradual phase transformation starting at 600-650K was clearly evidenced. A phase transition temperature of 773±25K has been reported by ferromagnetic NMR in micron size Co particles but it relied on a different assignment of the resonance lines.[21] Furthermore, Co is well known to have a phase transition from hcp to fcc at ~ 693K in bulk Co. The main result of the present study is thus that supported nanosize Co metal particles have a lower phase transition temperature (600-650K) than bulk or micron size cobalt metal (700-750K). Complementarily, according to Figure 7, at 850K, about 20% of the NMR intensity was still due to nuclei in hcp. Thus, despite the fact that the phase transformation had started at 600K, there was still no full hcp to fcc Co conversion at 850K. According to previous works,[20] the hcp phase fully disappears at ~ 700K in bulk cobalt. However, Kitakami et al. established theoretically that small fcc crystals can remain stable at room temperature.[28] Reversing the arguments, the stability of small hcp crystals at high temperatures can be expected.

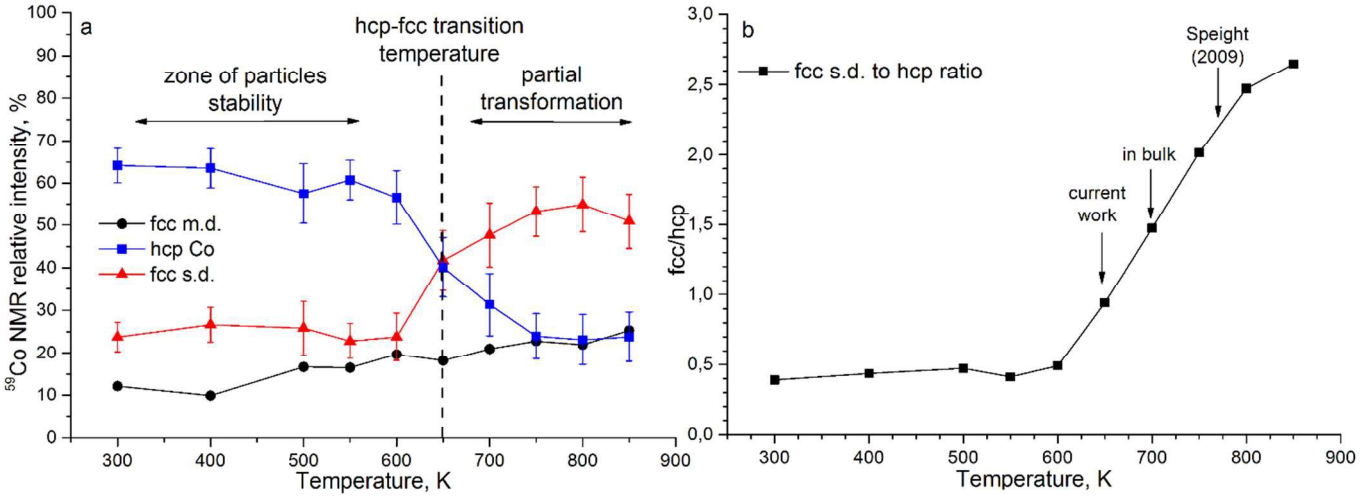

Figure 7. (a) Plot versus temperature of the relative integrated intensities obtained by decomposition of the lines of Figure 1. Blue squares correspond to the relative contribution of hcp Co, red triangles to fcc single-domain Co and black circles to fcc d.w. Co. The error could not be estimated for the fcc d.w. because the shape of the corresponding line is not Gaussian especially for temperatures below 650K. (b) Fcc/hcp ratio plotted versus temperature. The ratio was calculated by dividing fcc domains line by the hcp Co line since only these two lines participate in the transformation (the fcc m.d. relative contribution remained roughly constant).

Journal Name

ARTICLE

Interestingly, the fcc multi-domain resonance intensity was basically unaffected by temperature. This might mean that particles larger than the critical size of Co metal single-domain particles, namely ~ 50-70 nm,[24,51] were more stable with respect to the allotropic hcp-fcc phase transition with temperature. This interpretation remains debatable though as the intensity of lager particles might simply be related to a higher superparamagnetic transition temperature.

Conclusions

The present study shows by ferromagnetic ^{59}Co NMR the temperature behaviour of Co metal nanoparticles supported on β-SiC. The resonances of the fcc m.d. particles, fcc single-domain particles and hcp Co particles were clearly distinguishable. The allotropic transition was found to start in the 600-650K temperature range, that is 50K less than in the bulk and approximately 100K lower than in Co metal powders according to Speight et al.[21] A significant part of the sample remained in the hcp phase at the highest temperature considered (850K). The hcp-fcc transformation appeared fully reversible in the 300-850K temperature range.

Beyond these qualitative observations, a quantitative analysis requires a full description of the resonance behaviour with temperature. While the temperature – frequency dependence of all species could be well fitted by the two first terms of spin-waves theory, prediction of the dependence of the intensity on temperature was not possible at this stage, as the enhancement factor dependence on temperature is not known from a theoretical perspective. Quantitative analysis would have required a systematic empirical examination of the dependence of the spectrum intensity with the applied rf power, and this at all temperatures. This added complication resulted from the fact that the present study dealt with the ferromagnetic NMR spectra of cobalt nanoparticles *in situ*, contrarily to the study of Speight et al.[21] where the samples were quenched to room temperature before measurements. Indeed, our observation of particle stability up to 600K is relevant to many experimental situations, including but not restricted to the FTS catalytic processes.[9,11,27,32] Our description of the Co particles stability in temperatures near operando, up to 600K, might prove useful to understand and model active species in other catalytic or battery materials were the active species are above the superparamagnetic critical size.

Finally, the anomalous stability of some hcp domains up to 850K (the maximal temperature implemented in the present study) had never been reported before.

Acknowledgements

The authors thank Prof. V.I. Zaikovskii and PhD S.V. Cherepanova for providing HRTEM and XRD results. Anonymous reviewers must also be thanked for constructive comments. The sample preparation and treatment is supported by RAS project V.44.1.17. The NMR study is made possible by grant RFBR # 14-03-31684. Also A.S. Andreev thanks a doctoral grant from the French Embassy in Moscow and Zamaraev fund for a travel grant.

Notes and references

1 A. Y. Khodakov, W. Chu and P. Fongarland, *Chem. Rev.*, 2007, **107**, 1692–1744.
2 M. Tijmensen, *Biomass and Bioenergy*, 2002, **23**, 129–152.
3 M. M. Wright, R. C. Brown and A. A. Boateng, *Biofuels, Bioprod. Biorefining*, 2008, **2**, 229–238.
4 H. M. Torres Galvis and K. P. de Jong, *ACS Catal.*, 2013, **3**, 2130–2149.
5 B. Buragohain, P. Mahanta and V. S. Moholkar, *Energy*, 2010, **35**, 2557–2579.
6 T. V. Malleswara Rao, X. Dupain and M. Makkee, *Microporous Mesoporous Mater.*, 2012, **164**, 148–163.
7 7N. E. Tsakoumis, M. Rønning, Ø. Borg, E. Rytter and A. Holmen, *Catal. Today*, 2010, **154**, 162–182.
8 A. Jean-Marie, A. Griboval-Constant, A. Y. Khodakov and F. Diehl, *Comptes Rendus Chim.*, 2009, **12**, 660–667.
9 B. de Tymowski, Y. Liu, C. Mény, C. Lefèvre, D. Begin, P. Nguyen, C. Pham, D. Edouard, F. Luck and C. Pham-Huu, *Appl. Catal. A Gen.*, 2012, **419-420**, 31–40.
10 B. Lee, H. M. Koo, M.-J. Park, B. Lim, D. J. Moon, K. J. Yoon and J. W. Bae, *Catal. Letters*, 2012, **143**, 18–22.
11 Y. Liu, B. de Tymowski, F. Vigneron, I. Florea, O. Ersen, C. Mény, P. Nguyen, C. Pham, F. Luck and C. Pham-Huu, *ACS Catal.*, 2013, **3**, 393–404.
12 A. R. de la Osa, A. de Lucas, L. Sánchez-Silva, J. Díaz-Maroto, J. L. Valverde and P. Sánchez, *Fuel*, 2012, **95**, 587–598.
13 A. N. Murty, A. A. Williams, R. T. Obermyer and V. U. S. Rao, *J. Appl. Phys.*, 1987, **61**, 4361–4363.
14 A. N. Murty, M. Seamster, A. N. Thorpe, R. T. Obermyer and V. U. S. Rao, *J. Appl. Phys.*, 1990, **67**, 5847–5849.
15 M. J. Ledoux, O. Michaux, G. Agostini and P. Panissod, *J. Catal.*, 1985, **96**, 189–201.
16 P. Tolédano, G. Krexner, M. Prem, H.-P. Weber and V. Dmitriev, *Phys. Rev. B*, 2001, **64**, 144104.
17 C. R. Houska, B. L. Averbach and M. Cohen, *Acta Metall.*, 1960, **8**, 81–87.
18 H. L. Gaigher and N. G. van der Berg, *Electrochim. Acta*, 1976, **21**, 45–49.
19 J.-E. Bidaux, R. Schaller and W. Benoit, *Acta Metall.*, 1989, **37**, 803–811.
20 M. Kawakami, T. Hihara and Y. Koi, *J. Phys. Soc. Jpn.*, 1972, **33**, 1591–1598.
21 R. Speight, A. Wong, P. Ellis, P. T. Bishop, T. I. Hyde, T. J. Bastow and M. E. Smith, *Phys. Rev. B*, 2009, **79**, 054102–1 – 054102–8.

22 E. A. Turov and M. P. Petrov, *Nuclear Magnetic Resonance in Ferro- and Antiferromagnets*, Jerusalem : Israel Program for Scientific Tr. (Halsted Pr. N.Y.), 1972.
23 E. Jędryka, M. Wójcik, S. Nadolski, H. Pattyn, J. Verheyden, J. Dekoster and A. Vantomme, *J. Appl. Phys.*, 2004, **95**, 2770–2775.
24 Y. D. Zhang, J. I. Budnick, W. A. Hines, S. A. Majetich and E. M. Kirkpatrick, *Appl. Phys. Lett.*, 2000, **76**, 94–96.
25 T. Thomson, P. C. Riedi, S. Sankar and A. E. Berkowitz, *J. Appl. Phys.*, 1997, **81**, 5549–5551.
26 A. A. Sidorenko, C. Pernechele, P. Lupo, M. Ghidini, M. Solzi, R. De Renzi, I. Bergenti, P. Graziosi, V. Dediu, L. Hueso and A. T. Hindmarch, *Appl. Phys. Lett.*, 2010, **97**, 162503–162509.
27 A. S. Andreev, O. B. Lapina, J.-B. d'Espinose de Lacaillerie and A. A. Khassin, *J. Struct. Chem.*, 2013, **54**, S102–S110.
28 O. Kitakami, H. Sato, Y. Shimada, F. Sato and M. Tanaka, *Phys. Rev. B*, 1997, **56**, 13849–13854.
29 C. Rosant, B. Avalle, D. Larcher, L. Dupont, A. Friboulet and J.-M. Tarascon, *Energy Environ. Sci.*, 2012, **5**, 9936.
30 J. Cabana, L. Monconduit, D. Larcher and M. R. Palacín, *Adv. Mater.*, 2010, **22**, E170–92.
31 A. S. Andreev, S. F. Tikhov, A. N. Salanov, S. V Cherepanova, O. B. Lapina, V. A. Bolotov, Y. Y. Tanashev, J.-B. d'Espinose de Lacaillerie and V. A. Sadykov, *Adv. Mater. Res.*, 2013, **702**, 79–87.
32 Y. Liu, J. Luo, M. Girleanu, O. Ersen, C. Pham-Huu and C. Meny, *J. Catal.*, 2014, **318**, 179–192.
33 W. Hines, J. Budnick, D. Perry, S. Majetich, R. Booth and M. Sachan, *Phys. Status Solidi B*, 2011, **248**, 741–747.
34 Y. Y. Tong, *J. Magn. Res.*, 1996, **119**, 22–28.
35 A. S. Andreev, PhD thesis. Novosibirsk State University; Boreskov Institute of Catalysis, pp 147 (in Russian).
36 A. M. Portis and A. C. Gossard, *J. Appl. Phys.*, 1960, **31**, S205–S213.
37 A. C. Gossard and A. M. Portis, *Phys. Rev. Lett.*, 1959, **3**, 164–166.
38 A. C. Gossard, A. M. Portis, M. Rubinstein and R. H. Lindquist, *Phys. Rev.*, 1965, **138**, A1415–A1421.
39 H. Yasuoka and R. T. Lewis, *Phys. Rev.*, 1969, **183**, 559–562.
40 V. V Matveev, D. A. Baranov, G. Y. Yurkov, N. G. Akatiev, I. P. Dotsenko and S. P. Gubin, *Chem. Phys. Lett.*, 2006, **422**, 402–405.
41 A. S. Andreev, O. B. Lapina and S. V. Cherepanova, *Appl. Magn. Reson.*, 2014, **45**, 1009–1017.
42 S. G. Bailey, D. C. Creagh and G. V. H. Wilson, *Phys. Lett. A*, 1973, **44**, 229–230.
43 Y. Koi, A. Tsujimura and Y. Yukimoto, *J. Phys. Soc. Jpn.*, 1960, **15**, 1342.
44 M. Kawakami and H. Enokiya, *J. Phys. Soc. Jpn.*, 1986, **55**, 4038–4043.
45 C. Searle, H. Kunkel, S. Kupca and I. Maartense, *Phys. Rev. B*, 1977, **15**, 3305–3308.
46 H. P. Kunkel and C. W. Searle, *Phys. Rev. B*, 1981, **23**, 65–68.
47 W. Marshall, *Phys. Rev.*, 1958, **110**, 1280–1285.
48 E. C. Stoner, *Proc. R. Soc. London. Ser. A. Math. Phys. Sci.*, 1938, **165**, 372–414.
49 M. Weger, E. L. Hahn and A. M. Portis, *J. Appl. Phys.*, 1961, **32**, S124–S125.
50 M. Takahashi and T. Suzuki, *Jpn. J. Appl. Phys.*, 1979, **18**, 1071–1078.
51 D. L. Leslie-Pelecky and R. D. Rieke, *Chem. Mater.*, 1996, **8**, 1770–1783.